

Chapter 5

Mass Transfer and Mixing Across the Scales in Animal Cell Culture

Alvin W. Nienow

Abstract As in all aerobic bioprocesses, the oxygen transfer rate is a critical parameter that needs to be met for the satisfactory cultivation of animal cells. Oxygen in solution has to be continuously provided because of its low solubility in aqueous solution which is continually being utilised by the growing cells (at the current time, reaching a cell density of $\sim 10^7$ cells mL⁻¹ in bioreactors up to 25 m³). Such a process requires a certain specific power input (or mean specific energy dissipation rate) to be used, which also has to provide a satisfactory level of other mixing parameters. However, though for animal cells, the specific power required is relatively low (typically $< \sim 0.05$ W/kg), because of the lack of a cell wall, there is still a perception that ‘shear damage’ may occur. Another aspect of oxygen mass transfer is the need to provide a continual inflow of oxygen into the bioreactor, typically by sparging (rates $< \sim 0.01$ vvm). However, especially at large scale, sparging may lead to excessive foaming requiring the use of antifoam to control it; and bursting bubbles damage cells unless protective agents are used. Both these additives negatively affect the rate of mass transfer. Another critical aspect directly linked to oxygen transfer is the molar equivalent production of carbon dioxide by the cells. Stripping of CO₂ is essential to prevent physiologically damaging levels of pCO₂ being produced as well as issues associated with pH and osmolality. Essentially, oxygen transfer, carbon dioxide stripping and mixing parameters are all intimately connected and need to be considered in an integrated way. In this chapter, oxygen mass transfer and carbon dioxide stripping theory and practice are considered in detail including non-stirred and single use bioreactors. In addition, other mixing parameters such as blending, heat transfer and scale-up/scale-down in stirred bioreactors are briefly considered as these are used commercially from the 15 mL ambrTM to the 25 m³ scale. Because the perceived ‘shear-sensitivity’ of animal cells to stirring and bubbling has impacted on how aeration and stripping have been addressed in practice, these topics too are worthy of consideration in any integrated approach. Finally, some recommendations regarding sparger selection and impeller choice are also made.

A.W. Nienow (✉)

Department of Chemical Engineering, University of Birmingham, Birmingham, UK

Centre for Biological Engineering, Loughborough University, Loughborough, UK

e-mail: A.W.Nienow@bham.ac.uk

Keywords Oxygen transfer • Carbon dioxide stripping • ‘Shear damage’ • Mixing • Agitator selection • Sparger design • Scale-up/scale-down

5.1 Introduction

Stirred bioreactors have become the bioreactor of choice for most animal cell culture processes and with the growing popularity of the microbioreactor, ambrTM (Fig. 5.1 (TAP Biosystems, UK)) for clone selection and process optimization, etc., at all scales for both sterilisable and single use bioreactors. Though other single use bioreactors have also entered the field, particularly the wave-type, many of the principles by which cells are grown successfully in them are the same. Therefore this chapter will concentrate on mass transfer and mixing in stirred bioreactors; that is bioreactors in which rotating stirrers are present as the main energy source for achieving all the different processes that constitute mixing. Mixing involves a range of physical phenomena that are dependent on the rate of energy input by the rotating impellers such as homogenizing (blending) the liquid phase, achieving adequate heat transfer and dispersing sparged air into smaller bubbles thereby ensuring adequate oxygen transfer into the media and CO₂ stripping from it. Typically with aerobic processes, it is the rate of oxygen transfer that sets the specific power input (equivalent to the mean specific energy input rate), which is then dissipated in the bioreactor. Therefore, it is a major determinant of all the mixing processes occurring in it.

The special feature of animal cell culture because the cells lack a wall is the perception that this specific energy dissipation rate may damage the cells by

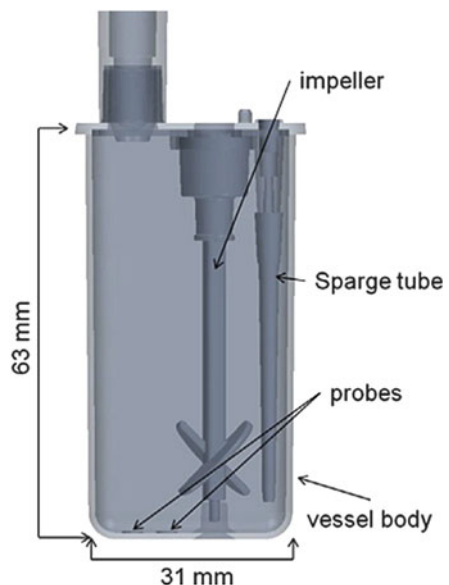


Fig. 5.1 15 mL ambrTM stirred bioreactor (depth 18 mm) (Adapted from Nienow et al. 2013a)

Table 5.1 Physical phenomena in stirred bioreactors for animal cell culture important for analyzing mass transfer and mixing across the scales

(a) Reynolds number, $\rho ND^2/\mu$ to establish flow regime
(b) Mass transfer coefficients, $k_L a$
(c) Un-aerated power draw, P (W) [or mean specific energy dissipation rate, $\bar{\epsilon}_T$ (W/kg) or specific power, $P/\rho V$ (W/kg)]
(d) Aerated power draw, P_g (W) or specific power, $P_g/\rho V$ (W/kg)
(e) Local specific energy dissipation rate, ϵ_T (W/kg) including the maximum near the impeller ($\epsilon_{T\max}$ (W/kg))
(f) Liquid-phase mixing time, θ_m (s)
(g) Gas-phase mixing (plug flow or back-mixed)
(h) Flooding–loading transition

inhibiting growth and/or productivity or changing the quality of the product. An integrated approach to mass transfer and mixing in cell culture must also include air sparging and dispersion which is essential for meeting the oxygen demand at the high cell densities now being produced (10^7 cells mL⁻¹ or more); and again the possibility of damage to cells from sparging (see Table 5.1).

Since mixing and mass transfer are physical phenomena, they can initially be studied without the complexity of actually growing cells. The type of information needed is also listed in Table 5.1 and it is important to know how changes of scale affect these parameters too. For animal cell culture, since the oxygen demand is relatively low compared to bacterial fermentations even at the current cell densities being achieved, the rate of specific energy input and dissipation is also low. An important fluid dynamic consideration which is critical for all the parameters in Table 5.1 is the Reynolds number, Re , defined as

$$Re = \rho ND^2/\mu \quad (5.1)$$

For $Re > \sim 10^4$, the flow in a bioreactor is turbulent. Therefore, as shown below, in most bioreactors for growing animal cells, where the physical properties of the media are similar to water, from the bench scale upwards in scale, the flow is turbulent. Thus, the phenomena in Table 5.1 need to be obtained under these conditions. It also important to know how the cells respond to turbulent flow under the agitation and sparging conditions typical of bioreactors (Nienow 2014).

Since this chapter is particularly concerned with mass transfer, it will be considered in detail first. However, since mass transfer depends on the mean specific energy dissipation and sparge rate, both of which affect the various mixing topics in Table 5.1 and give rise to concern regarding hydrodynamic stress on cells, these aspects are also considered somewhat briefly. Finally, since many of the data obtained at smaller less expensive scales of operation are then used in the design and operation of commercial cell culture bioreactors, consideration of scale-up/scale down is included again briefly for completeness.

5.2 Oxygen Mass Transfer

To meet the oxygen demand of the cells (OD), oxygen has to be continuously supplied because of its limited solubility in the media. In the case of animal cells, the specific oxygen demand (SOD), which is independent of scale, is low (typical values of about 10^{-16} to 10^{-17} mol s $^{-1}$ cell $^{-1}$ (Nienow et al. 1996; Xing et al. 2009) for CHO cells) and though cell density, X , has steadily increased over the years to about 10^7 cells mL $^{-1}$, relative to many other organisms, the overall $OD = (SOD \cdot X)$ is also low. Provided the cell density achieved is the same across the scales, then so is the OD . This low OD means that the oxygen transfer rate required is low and therefore because it is linked to the specific power input from the agitator when aerated, $P_g/\rho V$, is also typically low ($< \sim 0.075$ W kg $^{-1}$) as is the sparge rate ($< \sim 0.01$ vvm) (Nienow 2006). These factors impact on the way the basic mass transfer model is modified in order to calculate the mass transfer coefficient from the basic mass transfer equation which will now be addressed.

5.2.1 Basic Oxygen Mass Transfer Concepts and Equations

Figure 5.2 shows the steps by which oxygen passes from a bubble at a partial pressure p_g (partial pressure of oxygen in air, oxygen-enriched air or pure oxygen also allowing for back pressure) to the animal cell. The steps consist of transport through the gas film inside the bubble, across the bubble-liquid interface, through the liquid film around the bubble, across the well-mixed bulk liquid (media plus product in solution) through the liquid film around the cell where it is utilized within the cell. Each step offers a resistance to oxygen transfer; and each step itself is dependent on the mass transfer coefficient for that step, the area available over which mass transfer can occur and the relevant driving force. For very small entities

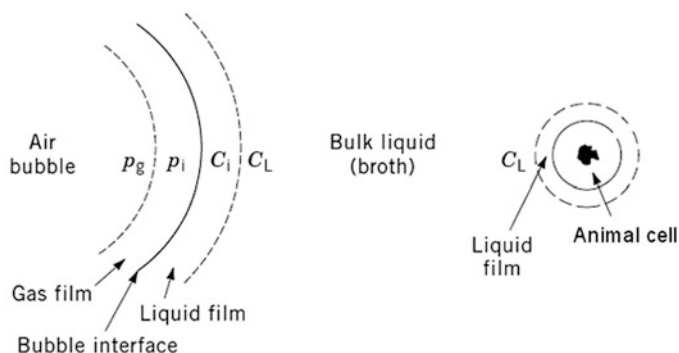


Fig. 5.2 Oxygen mass transfer steps

like animal cells, the mass transfer coefficient is very high (Nienow 1997a) and the specific surface area, a_p (both $\propto 1/\text{particle size}$) is very large so that step is very fast.

At the gas liquid interface, the area is the same for both the gas film and the liquid film but the mass transfer coefficient increases with an increase in the diffusion coefficient. Since the latter is much higher for the gas phase than for the liquid, the rate limiting step is in the liquid film. In addition, as a result, $p_g \approx p_i$. In addition for all mass transfer processes, it is assumed that equilibrium exists at the interface between the two phases. This assumption implies that, at the interface, the concentration of the gas in the liquid, C_i , is equal to its solubility at its partial pressure in the gas phase, p_i . Since, for sparingly soluble gases such as oxygen, there is a direct proportionality between the two,

$$p_i = HC_i \quad (5.2)$$

where H is the Henry's law constant.

The rate of mass transfer, J , at the gas liquid-interface is then assumed to be proportional to the concentration differences existing within each phase, the surface area between the phases, A , and a coefficient (the gas or liquid film mass transfer coefficient, k_g or k_L , respectively) which relates the three. Thus

$$J = k_g A (p_g - p_i) = k_L A (C_i - C_L) \quad (5.3)$$

and

$$C_i = p_i/H = p_g/H = C_g^* \quad (5.4)$$

where C_g^* is the solubility of oxygen in the media that is in equilibrium with the gas phase partial pressure of oxygen. Thus the aeration rate per unit volume of bioreactor, N , is given by

$$N = J/V = k_L (A/V) (C_g^* - C_L) = k_L a (C_g^* - C_L) \quad (5.5)$$

where a is the specific area of bubbles. Thus, for satisfactory operation, the maximum oxygen demand of the cells (OD_{max}) must be met and it is related to the maximum cell concentration (X_{max}) by

$$OD_{max} = SOD \cdot X_{max} \quad (5.6)$$

Thus, for stable operation, OD (or Oxygen Uptake Rate, OUR) needs to be met by the oxygen transfer rate, OTR . Thus,

$$OD_{max} = OUR_{max} = OTR = k_L a (C_g^* - C_L) = k_L a \Delta C_L \quad (5.7)$$

For satisfactory operation, $C_L > (C_L)_{crit}$ where $(C_L)_{crit}$ is the critical oxygen concentration below which the performance of the bioreactor begins to deteriorate

whilst above it, the performance is zero order with respect to dissolve oxygen concentration, i. e. independent of it. It may in some cases, need to be below some upper level that inhibits growth. Neither the upper or lower levels have been well established for animal cells though values between 5 % and 95 % of saturation with respect to oxygen in air (between 5 % and 95 % dO_2) have been reported not to have any impact on cell growth (Nienow 2006). Nevertheless, it is more common to try to control dO_2 in the range 30–50 % of saturation.

C_g^* depends on the partial pressure of oxygen in the gas phase, p_g and this can be related to the total pressure, P_g from Dalton's law of partial pressures

$$p_g = P_g y \quad (5.8)$$

where y is the mole (volume) fraction of oxygen in the gas phase and P_g is the total pressure, i. e. back pressure plus static head. C_g^* is also a function of the liquid composition (and is lower in solutions containing electrolytes than in pure water) and reduces with increasing temperature. Thus the driving force for mass transfer can be increased by enhancing C_g^* ; and lowering C_L provided it is $> C_{crit}$. However, in a large scale bioreactors (which may be up to 25 m³) where circulation times of the liquid are sufficient for significant oxygen depletion by the respiring cells (Sweere et al. 1987), the average value may need to be kept well above C_{crit} so that local values below it can be avoided. Hence, the choice of values in the range 30–50 %.

Nevertheless, in a stirred bioreactor, the liquid is generally considered well-mixed, i. e. C_L is spatially constant. This is a reasonable assumption for the liquid phase in animal cell culture except at the larger scales. The measurement of the local concentration is done by a polarographic electrode and the reading obtained is dependent on the velocity over the probe. Since the velocity varies so much, establishing the exact concentration field is generally not possible. Assumptions also have to be made regarding the mixing of the gas phase. It may be well mixed so that

$$p_g = constant = (p_g)_{out} \quad (5.9)$$

where $(p_g)_{out}$ is the partial pressure of oxygen in the exit gas and

$$C_g^* = (p_g)_{out} / H \quad (5.10)$$

On the other hand, for ease of determining $k_L a$ from experimental data, it is often assumed that the gas is well mixed and $p_g = (p_g)_{in}$, i.e. no oxygen is utilized. This is the so-called no-depletion model. In this case,

$$C_g^* = (p_g)_{in} / H \quad (5.11)$$

For larger-scale bioreactors (Pedersen 1997), the gas phase is generally considered as being in plug flow, so that a log mean value of driving force is obtained, ΔC_{\log} :

$$\Delta C_{\log} = \Delta C_{in} - \Delta C_{out} / \ln(\Delta C_{in} / \Delta C_{out}) \quad (5.12)$$

where

$$\Delta C_{in} = (p_g)_{in} / H - C_L \quad (5.13)$$

and

$$\Delta C_{out} = (p_g)_{out} / H - C_L \quad (5.14)$$

The assumption made is not very important in cell culture except at large scale and high cell densities because the amount of oxygen removed compared to that introduced is quite small. On the other hand it is very important in high oxygen demanding bacterial and mycelial fermentations.

5.2.2 The Volumetric Mass-Transfer Coefficient, $k_L a$

In bioreactors with pipe or ring spargers, the bubble size generated which controls a and the mass transfer coefficient, k_L both are largely dominated by bubble break-up in the impeller region. Because of this close connection with agitation and the difficulty of linking either to fundamental fluid dynamic phenomena, there is little to be gained by separating them in this article. However, both are dependent on agitation intensity usually best considered as specific energy dissipation rate, ε_T and significantly, liquid composition. In general, both solutions and suspensions reduce the mobility of the bubble interface thereby reducing the ease with which oxygen can pass across the interface (Davies 1972; Prins and van't Riet 1987; Sieblist et al. 2013) and, consequently, the value of k_L . However, electrolytes and alcohols also reduce the mean bubble size, usually denoted as d_{32} , the Sauter mean diameter. The latter is the mean bubble size giving the same volume/surface area ratio as the whole gas hold-up in the bioreactor, ε_G given by

$$\varepsilon_G = (H_G - H) / H_G \quad (5.15)$$

where H_G is the height of liquid in the bioreactor during aeration and H is the height without aeration. Thus, the bubble size, hold-up and the specific interfacial area between the two phases, a , are related by

$$d_{32} = 6\varepsilon_G/a \quad (5.16)$$

Clearly, smaller bubbles individually have a higher specific surface area but they also tend to circulate more with the liquid motion thus giving a higher hold up with both factors increasing a and thus $k_L a$.

These two opposing effects (the additive lowering k_L but enhancing a) make the prediction of $k_L a$ very difficult. Thus, in the media for animal cell culture, Pluronic F68 has to be present if sparged aeration is employed in order to prevent fluid dynamic stress from bursting bubbles from damaging the cells (Nienow 2006); and with pipe or ring spargers, it lowers k_L by a factor of 2–3 (Sieblist et al. 2013). It also caused a reduction in $k_L a$ with sinter-type (Sieblist et al. 2013). Antifoam has a similar effect in media (Lavery and Nienow 1987; Morao et al. 1999) and during actual cultivation when it is often essential in order to prevent excessive foaming (Mostafa and Gu 2003).

On the other hand, electrolytes and alcohols both lead to significant reductions in bubble size. In some ways, this similarity is surprising since some theoretical correlations suggest that bubble size is reduced by reducing surface tension. However, this theoretical approach assumes that the bubble size is dependent only on break-up whilst in fact the equilibrium size depends on the competing mechanisms of break-up and coalescence. Thus, even though the surface tension of salt solutions is slightly higher than water and the presence of alcohols lowers it by a factor of about 2, in both cases, bubble size is smaller than in water. It is the way the electrolyte ions or the hydrophilic part of the alcohol align themselves at the bubble-solute interface which causes electrostatic surface charges and these in turn hinder coalescence. In that case, the combined effect is an increase in $k_L a$ (Machon et al. 1997; Hu et al. 2007).

The main reason for this increase is because when the bubbles are smaller, bubbles circulate more easily which leads to a larger hold-up, ε_G with increasing agitation intensity and hence specific surface area, a (Eq. 5.15). Since agitation only has a weak impact on bubble size in sparged systems (Takahashi and Nienow 1991) and there is a strong physical linkage between bubble size and hold up, ε_G and $k_L a$ are often related to agitation and aeration rate in similar ways. However, exceptions to this interrelationship have been reported (Martin et al. 1994) and therefore it should be treated with care. For example, if a certain agitator produces a higher hold-up without a commensurate increase in $k_L a$, it represents a reduction in performance because productivity is linked to the volume of broth in the fermenter.

Finally, it should be note that $k_L a$ is temperature dependent, the relationship being:

$$(k_L a)_T = (k_L a)_{20} \alpha^{(t-20)} \quad (5.17)$$

where $(k_L a)_{20}$ is the value at 20 °C, $\alpha \approx 1.022$, and t is the temperature, °C; i.e. $k_L a$ increases by $\sim 2.5\%$ /C.

5.2.3 The Measurement of k_La

There are two main methods for measuring k_La , the unsteady-state and the steady-state method. Each has different advantages and weaknesses and both may give inaccurate results if the polarographic probe or fluorescent optical patch is not in a region of high liquid velocity so that the local dO_2 at the surface of the probe is not depleted. If the velocity is low, erroneous low dO_2 readings may be obtained.

5.2.3.1 The Unsteady-State (Dynamic) Method

The unsteady-state (also known as dynamic) technique is the most common because at first sight it appears very simple. Basically, the level of dissolved oxygen is first reduced to zero (or close to it), either by bubbling through nitrogen or by adding sodium sulfite (van't Riet 1979). Then, after switching to air sparging, the increase in dissolved oxygen concentration as a function of time is followed using a polarographic oxygen electrode or more recently for animal cell culture, a fluorescent dissolved oxygen probe of the type made by Precision Sensing GmbH, Germany (Nienow et al. 2013a; Sieblist et al. 2013).

However, potentially, it is very difficult to get accurate k_La data using the dynamic technique. Firstly, one of the assumptions set out earlier about the extent of gas-phase mixing has to be made and the choice can be very significant, giving when k_La values are high values differing by an order of magnitude for the same raw data depending on the assumption made (Linek et al. 1987; Nienow 2003a). Secondly, the electrode or patch response time also has to be relatively fast so that

$$\tau_p \ll 1/5k_La \quad (5.18)$$

(van't Riet 1979) if a correction for the true dO_2 compared to that on the probe is to be neglected. At high k_La as found in many bacterial fermentations, correction is nearly always required. Finally, the assumption that the liquid phase is well mixed (i.e. the dO_2 is the same at all locations) is often not satisfied especially at large scale and high k_La values. In fact, certain papers have ignored this requirement and where oxygen electrodes have given different reading at various locations have used the data to give local k_La values (Lu et al. 2002). Such values are completely erroneous, of course (Nienow 2003b). To get local k_La values experimentally, the liquid phase mixing itself has to be modeled by subdividing it into one or more well-mixed regions associated with different impellers and the exchange flow rate between them must be estimated (Vasconcelos et al. 1997).

Fortunately, these problems associated with the unsteady, dynamic technique are greatly reduced for animal cell culture. The maximum k_La values required to satisfy the oxygen demand of cell cultures up to 10^7 cells/ml is about 15 h^{-1} and even though the sparge rate is low (~ 0.01 vvm), the depletion of the gas phase is quite small, so the no depletion model can be used with a satisfactory degree of accuracy.

In addition, the response time of electrodes or patches is $\ll 1/5k_La$ and so it can be neglected. Therefore, the basic equation that needs to be solved is

$$OTR = dc_L dt = -k_L a \cdot (C_g^* - C_L) \quad (5.19)$$

The no-depletion model allows this to be simply integrated because C_g^* can be assumed constant in equilibrium with the inlet gas composition at all times. This gives

$$k_L a (t - t_0) = \ln \left(\frac{C_g^* - C_L}{C_g^* - C_{L,0}} \right) \quad (5.20)$$

where the subscript 0 refers to the time at which the initial liquid phase dO_2 for the experiment was measured or utilized for the calculation of $k_L a$. Expressing this equation in terms of the % dissolved oxygen, $X\%$, concentration from the measurement gives

$$k_L a = \ln(100 - X/100 - X_0)/\Delta t \quad (5.21)$$

$k_L a$ is then usually obtained by expressing the results on a semi-log plot using data from around 20 % to 80 % dO_2 . If the dO_2 is reduced to zero, the equation can be rearranged to give

$$X = 100 - \exp[-t/(1/k_L a)] \quad (5.22)$$

From here it can be seen that when $t = 1/k_L a$, $X = 63\%$. This method gives a very quick way of obtaining a ball-park figure for $k_L a$.

As already pointed out, $k_L a$ is very sensitive to the precise composition of the liquid phase. Thus, the $k_L a$ of distilled water after reducing dO_2 to zero by nitrogen degassing is significantly less than that obtained if sulfite deoxygenation is used. This difference occurs because the sulfite acts as a coalescence inhibitor, greatly reducing the bubble size and enhancing hold-up, and therefore increasing a and $k_L a$. Even the $k_L a$ in an actual cell culture is generally not identical to that obtained in any cocktail of chemicals which aim to mimic it such as the actual culture media including Pluronic F68 plus antifoam. The latter is commonly used and is the best approximation available. However, the dynamic technique can be adapted to work on an actual cultivation (Bandyopadhyoy et al. 1967; Langheinrich et al. 2002) which represents a significant advantage for the dynamic method.

5.2.3.2 The Steady State Technique

In the steady state method, Eq. 5.5 is utilized. One method for obtaining the OUR is to use a real culture and base it on the difference between the air concentration in the inlet air and that in the exit; and on the airflow rate. Provided the fall of oxygen

concentration is sufficient, this approach also enables the change of k_La with time and agitation conditions during the fermentation to be monitored (Albaek et al. 2011). However, for animal cell culture, the difference in oxygen concentration between inlet and outlet is usually insufficient to give accurate results. Another approach is to use a suitable mimic media plus catalase as a catalyst to break down hydrogen peroxide which is pumped into the bioreactor. Thus oxygen is generated in solution and oxygen is in fact stripped from the fluid (Cooke et al. 1991; Gezork et al. 2001). For both techniques assumptions have to be made about Henry's law constant, H which is required in order to obtain C_g^* ; H , like k_La , is also rather sensitive to composition. To the author's knowledge, the hydrogen peroxide technique has not been used for cell culture.

5.2.4 Correlations for Calculating k_La

5.2.4.1 Stirred Bioreactors

There are a very large number of correlations available in the literature for estimating k_La for sparged, stirred systems but the two equations developed from a survey by Van't Riet (1979) are still commonly used as bench marks. The equations are of the form,

$$k_La = A(\bar{\epsilon}_T)_g^\alpha (v_S)^\beta \quad (5.23)$$

where $(\bar{\epsilon}_T)_g$ is the mean specific energy dissipation rate, W/kg, (though it is also often expressed as kW/m³, the two being numerically equal in media of density = 1,000 kg/m³) from agitation and sparging and v_S is the superficial gas velocity (numerically equal to the volumetric sparged flow rate, Q_G (m³/s) divided by the cross-sectional area of the bioreactor). Critically, since this is a dimensional equation, the numerical value of A is dependent on the units used to express the parameters in Eq. 5.23. In addition, as already noted, since k_La is very sensitive to composition, A also depends on the properties of the fluid present in the bioreactor. With very viscous broths as found in mycelial fermentations for example, k_La falls significantly and a viscosity term with a negative exponent is included in Eq. 5.23. For the small variations in viscosity associated with media composition, anti-foam and Pluronic F68, any impact on k_La is taken into account in the constant A .

Van't Riet (1979) found that he could correlate a large amount of literature data (itself based on the 'no-depletion' assumption) in two equations of the form shown in Eq. 5.23. The first, for coalescing systems (mainly based on literature studies with water) gave $A = 2.6 \times 10^{-2}$, $\alpha = 0.4$ and $\beta = 0.5$ when the units of k_La are s⁻¹, of $(\bar{\epsilon}_T)_g$, W/m³ and of v_S , m/s. For non-coalescing systems (mainly based on electrolyte solutions) which have smaller bubbles, generally leading to higher k_La values compared to water, the constants $A = 2 \times 10^{-3}$, $\alpha = 0.7$ and $\beta = 0.2$. The

dimensional nature of this equation makes it somewhat unsatisfactory especially the impact of the units used for the various parameters but the most important points are that it was found to apply regardless of the impeller type and independent of scale.

The applicability of an equation of the form of Eq. 5.23 for stirred animal cell culture bioreactors was shown by Hoeks et al. (2004) for $k_L a$ in culture media across the scales for 0.012, 0.5 and 20 m³ bioreactors (Fig. 5.3). Langheinrich et al. (2002) showed similar $k_L a$ values at the same $(\bar{\epsilon}_T)_g$ and superficial air velocity during actual cell culture in 8 and 0.1 m³ bioreactors. In addition, in water, good agreement (with the appropriate constants) with the Van't Riet correlation for two different impeller types, even though the values of $(\bar{\epsilon}_T)_g$ and v_S used to give the original equation were an order of magnitude or more greater than in animal cell culture. In order to do so, Langheinrich et al. (2002) found that, because of the low specific energy dissipation rates associated with the agitation, inclusion of the specific energy dissipation rate from sparging ($=gv_S$ in W/kg) was particularly important. Lavery and Nienow (1987) also found the Van't Riet equation for water fitted their bench scale water data well.

A recent correlation for large scale $k_L a$ values measured by the dynamic technique was given by Xing et al. (2009). They mimicked a media (which included sodium chloride, sodium bicarbonate and 1 g/L Pluronic F68) used by Bristol-Myers Squibb for Chinese hamster ovary (CHO) cell culture at 3–4.4 m³ volume with a pipe sparger in a 5 m³ bioreactor. The equation was

$$k_L a = 0.075(P_g/V)^{0.47} v_S^{0.8} \quad (5.24)$$

where $k_L a$ is in s⁻¹, P_g/V in W m⁻³ and v_S in m s⁻¹. Since Eq. 5.23 was obtained under conditions that closely mimic those used during large-scale culture, it may be a good one to use (with caution) for such cases. On the other hand, the air flow rate used was surprisingly low (0.0013 vvm) which may explain why the exponent on v_S was so high. It is also interesting to note that P_g/V was rather high (up to 125 W m⁻³) and the maximum $k_L a$, rather low (<3.5 h⁻¹).

At the other size extreme, Nienow et al. (2013a) have measured $k_L a$, again using the dynamic method, in medium plus Pluronic F68 and antifoam (as well as water)

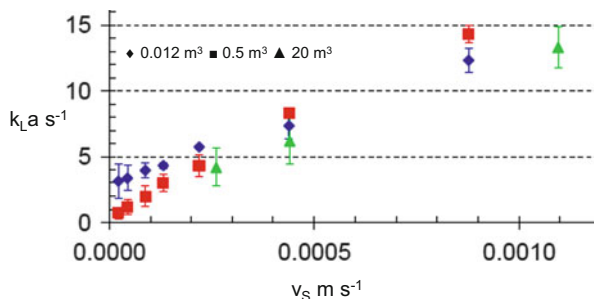


Fig. 5.3 $k_L a$ as a function of superficial gas velocity in cell culture bioreactors at three scales at constant mean specific energy dissipation rates (Adapted from Hoeks et al. 2004)

in the 15 mL ambrTM bioreactor (see Fig. 5.1). They found the values for both compositions surprisingly similar and for the mimicking mixture

$$k_L a = 1.74(P_g/V)(Q_G)^{0.15} \quad (5.25)$$

where $k_L a$ is in h^{-1} , P_g/V is in W m^{-3} and Q_G is in mL min^{-1} . Here, the vvm was very high (0.07 vvm) and the exponent on flow rate, low. However, because of the small scale, v_S was very low and therefore a high P/V (up to $\sim 500 \text{ W m}^{-3}$) was required to get $k_L a$ values up to 10 h^{-1} . These large variations in the flow rate expressed in different ways and in consequence specific power input/energy dissipation rate are a good example of the changes which take place when the variation of scales is very significant. Nevertheless, all the $k_L a$ values in the ambrTM were close to those predicted from the correlation of Van't Riet for coalescing (water) conditions, probably because the increase expected due to the presence of salts in the media are balanced by the reduction associated with antifoam and Pluronic. The use of the ambrTM in scale down studies is discussed again later in Sect. 5.9.

These correlations are not generally applicable when using sparging devices which control the bubble sizes, often called fritted spargers (Sieblist et al. 2010). Frits can be composed of Teflon, stainless steel, glass and other materials. Most often they are formed from small solid particles of the order of tens to a few hundred microns (often spheres) that are pressed into a shape and then sintered to form a stable porous wall. Usually, the sintered frits are closed tube elements or flat membranes characterized by their mean pore size, which depends on the size of the solid particles used to build the frit and the associated sintering process. As the solid material in the frit cannot be arranged regularly, the pore size distribution is rather broad so that the bubble sizes produced by them and therefore their mass transfer performance is somewhat variable from frit to frit of the same nominal size (Sieblist et al. 2010).

Mustafa and Gu (2003) using sparge stones found $k_L a$ values with a $10 \mu\text{m}$ sparge stone in a 1 m^3 bioreactor with antifoam were $5\text{--}10 \text{ h}^{-1}$, approximately double that with an open pipe (but without antifoam), whilst at the 1.5 L scale, the sparge stone gave $k_L a$ values without antifoam up to 180 h^{-1} when the open gave values up to $\sim 7.5 \text{ h}^{-1}$. Because the bubble size is controlled by the sparger, they found little increase in $k_L a$ with increasing impeller speed but an approximately proportional increase with increasing air flow rate. Sieblist et al. (2013) using sintered metal spargers measured bubble size of about 7 mm with a ring sparger and about 3 mm with a $47\text{--}100 \mu\text{m}$ metal sparger whilst photos of bubbles from a $25\text{--}47 \mu\text{m}$ one showed that they were very much smaller.

Clearly, the functionality found with such spargers is very different to those with open pipe and ring spargers and very dependent on the pore size. The small bubbles also are prone to cause foaming and Mustafa and Gu (2003) had to use antifoam at the 1 m^3 scale to prevent it at 0.002 vvm whilst foaming did not occur at 0.01 vvm with an open pipe sparger. Overall, the use of sintered spargers or sparge stones at the small scale leads to high $k_L a$ values at very low gas flow rates and agitation

intensities. As reported by Xing et al. (2009), this can lead to unsatisfactory designs at the large scale as such spargers lead to foaming; and inadequate agitation intensities with other sparger types lead to insufficient oxygen transfer. As discussed below, CO₂ stripping is also a potential issue.

For stirred single-use bioreactors (SUBs) with open pipe or ring spargers, the same type of functionality as that illustrated by the Van't Riet equation applies. Energy needs to be dissipated and air needs to be sparged if satisfactory mass transfer is to be achieved. The real question is, are these parameters large enough to achieve the k_La required for the cell density that could potentially be achieved? If yes, then the SUB will be satisfactory from an oxygen transfer perspective. If no, then the cell density achieved will be less than the maximum achievable and the performance less than optimum. If the oxygen demand is met by using a porous sparger, then the other issues arise.

5.2.4.2 Headspace Aeration and Shaken Bioreactors

If energy is imparted by rocking, rotation or shaking, then aeration occurs through the top surface as it does with headspace aeration in stirred bioreactors. For stirred bioreactors, $k_La \propto N^{0.6} \propto (\bar{\epsilon}_T)^{0.2}$; and it is also improved by placing the impeller close to the top surface. The use of dual impellers is therefore helpful and effective (Lavery and Nienow 1987). Nevertheless, the headspace k_La is only about 50 % of the sparged one at the bench scale. Similarly with the use of rocking or shaking motion, if it is vigorous enough (the energy input is sufficient to provide high enough velocities at the gas liquid interface or ingest enough bubbles by the action of waves), the k_La will be adequate (Oosterhuis et al. 2013) (which it is at the shake flask (Anderlei and Büchs 2001), spin tube (de Jesus et al. 2004) and microwell scale (Hermann et al. 2003; Betts et al. 2014) In general, unless the horizontal area is increased relative to the depth of the bioreactor when using headspace aeration, the specific area available for mass transfer falls with increasing scale ($\propto (1/\text{linear dimension for geometrically similar configurations})$). Hence, k_La should also fall, which makes the claimed performance for some large scale orbitally shaken bioreactors hard to understand (De Jesus and Wurm 2013). This change with scale increases the need to enrich the air with oxygen to increase the driving force and run the risk of pCO₂ build up as discussed below. The rate of airflow across the upper surface also has an impact but it does not represent a way of using air efficiently compared to bubbling aeration when agitating.

5.2.4.3 Bubble Columns

In the 1980s, it was considered bubble columns and airlift bioreactors were less likely than stirred ones to damage animal cells during culture (Varley and Birch 1999). However, once it became apparent that that bursting bubbles represented a

serious threat to cell viability, their use rapidly declined; even after the effectiveness of Pluronic F68 as protective agent became apparent. Nevertheless, they do offer a relatively simple way of providing oxygen transfer at rates which enable cells to grow and especially at the small scale, the use of Pluronic F68 should protect the cells.

For open pipe and ring spargers in water for a wide range of bubble column sizes based on the literature and their own work, Heinen and van't Riet (1982) found

$$k_L a = 0.32 v_S^{0.7} \quad (5.26)$$

which, when compared on a specific power basis, showed similar $k_L a$ values to those in agitated systems. Doig et al. (2005) worked with small bubble columns of 10 and 40 mm diameter with an aspect ratio of 2 and found a similar relationship between $k_L a$ and superficial gas velocity to that in Eq. 5.26. Specific power inputs up to 0.4 W/kg were generated leading to $k_L a$ values up to 300 s⁻¹. Clearly, bubble columns are capable of meeting the oxygen demands of cell culture, though the question of cell shear sensitivity to bubbling at scale still persists.

5.3 Carbon Dioxide Stripping

5.3.1 The 'Apparent' Mass Transfer Coefficient Issue

In principal, the basic equations for aeration (oxygen mass transfer) apply to carbon dioxide stripping (CO₂ mass transfer). However, in detail, they are very different. Firstly, the solubility of CO₂ at 25 °C and 1 bar is 33 mmol/L, more than two orders of magnitude greater than that of oxygen in air (0.2 mmol/L), i.e. Henry's Law constant is much smaller. Thus the application of the basic theory is different since that for oxygen is for a sparingly soluble gas whilst CO₂ is extremely soluble. As a result, when a bubble of air is passed through media depleted of oxygen but saturated with CO₂, it quickly fills (saturates) with the latter because of its high solubility so that the driving force at the start, very quickly becomes zero and no further CO₂ can be transferred. For oxygen, the concentration falls only slowly and it continues to supply O₂ as it rises as illustrated in Fig. 5.4.

The other parameter that determines the rate of mass transfer is k_L . Basic mass transfer theories suggest that $k_L \propto D_L^a$ where D_L is the mass diffusivity of the transferring species and $a = 1$ for the film theory of mass transfer and 0.5 for the penetration theory. Thus, since D_L is 1.92×10^{-9} m²/s for CO₂ in water at 25 °C and 2.1×10^{-9} m²/s for O₂, the difference should only be 5–10 %. This estimate of k_L for CO₂ based on k_L for O₂ is important because measuring $k_L a$ for CO₂ is difficult. Indeed, it is often done incorrectly using the unsteady state technique assuming that the gas composition does not change as it rises through a CO₂-saturated aqueous solution. i. e. equivalent to the no-depletion model for oxygen

Fig. 5.4 The change of oxygen and carbon dioxide concentration in a bubble of air as it rises through water saturated with CO₂ and stripped of O₂ due to the different solubility of the two gases (Adapted from Sieblist et al. 2011a)

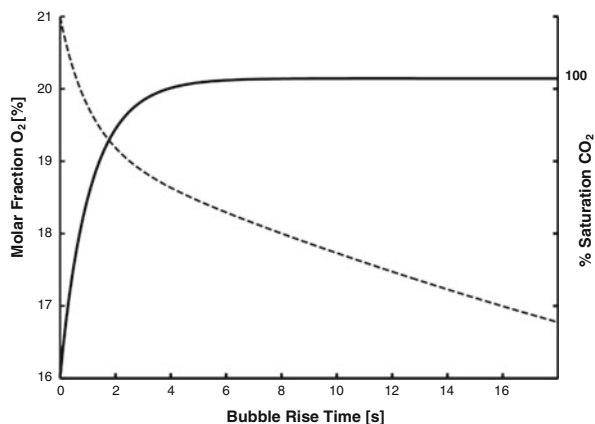
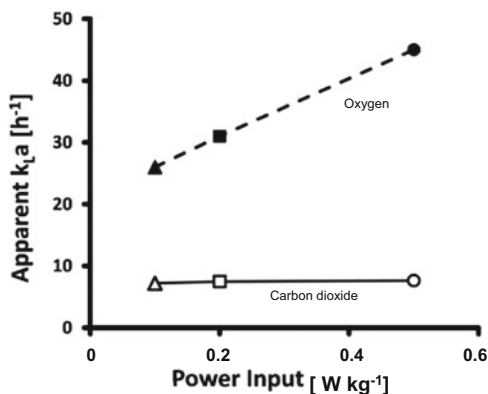


Fig. 5.5 ‘Apparent’ $k_L a$ as a function of the specific power input at a constant aeration rate for oxygen and carbon dioxide transfer (Adapted from Sieblist et al. 2011a)



transfer. However, as indicated above, the bubbles rapidly fill with CO₂ and the driving force for CO₂ mass transfer falls to zero. Since enhanced agitation intensity only leads to smaller bubbles and higher hold up, hence a longer residence time for bubbles in the vessel, agitation intensity has a minimal effect if any on the value of $k_L a$ (an ‘apparent’ $k_L a$) when measured this way. On the other hand, with increasing airflow, the bubbles even if they eventually become saturated remove more CO₂ so that the apparent $k_L a$ is enhanced. This relative impact of agitation and sparge rate on ‘apparent’ $k_L a$ is shown in Fig. 5.5.

5.3.2 CO₂ Evolution Rate, CER, and Control of pCO₂

At the initial stages of cultivation, it is necessary to control pH by sparging CO₂ in with the air, essentially along the lines first proposed by Telling and Stone (1964). Because of its high solubility, this mass transfer step is easily accomplished.

However, later in the culture, the CO_2 in solution can easily increase excessively. The respiratory quotient, RQ (mol CO_2 produced per mol O_2 consumed) for animal cell culture is approximately 1 (Ozturk 1996; de Zengotita et al. 2002). Thus for every mol of oxygen transferred into the media that is utilized by the cells, no matter whether this is achieved by higher $k_L a$ or higher driving force, a mol of CO_2 is produced. However, if the oxygen transfer is achieved at low sparge rates, for the reasons discussed above, CO_2 will not be stripped out of the media. Even so, because of the perceived ‘shear’ sensitivity of animal cells (discussed further below), low air flow rates are often used and oxygen transfer rates are maintained high by using a high oxygen driving force (oxygen enriched air or enhanced back pressure) or high $k_L a$ (using a fritted sparger to give small bubbles of high specific area, a).

High levels of pCO_2 of 150–200 mmHg levels have been reported in 1,800–2,500 L bioreactors and in high cell density perfusion bioreactors (Goudar et al. 2007) and detrimental effects have been reported at these levels for a number of systems; hybridoma, NSO and BHK cells (de Zengotita et al. 2002), CHO (Mostafa and Gu 2003) and insect cells (Garnier et al. 1996). De Zengotita et al. (2002) also showed that the cells they studied grew well in the range ~ 35 to ~ 80 mmHg pCO_2 , comparable to the physiological range of 31–54 mmHg pCO_2 .

The level of pCO_2 and the ability to strip it out is closely connected to the sparge rate in the following way. Assuming that the respiratory quotient, $RQ = 1$ and that the $k_L a$ for CO_2 and O_2 are the same, then

$$OUR = k_L a \Delta C_{\text{O}_2} = CER = k_L a \Delta C_{\text{CO}_2} \quad (5.27)$$

so that

$$\Delta C_{\text{O}_2} = \Delta C_{\text{CO}_2} \quad (5.28)$$

Assuming the dissolved oxygen is controlled at 40 % of saturation, then since in air there is only 21 vol.% oxygen, the partial pressure of oxygen is $760 \times 0.21 \times 0.4 = \sim 60$ mmHg. Thus $\Delta C_{\text{O}_2} = \sim 100$ mmHg. Therefore, ΔC_{CO_2} at the exit would also have to be ~ 100 mmHg. However, as shown above for many cells, the toxic level for CO_2 in solution is about 15–20 % of saturation, i. e. ~ 110 –150 mmHg, so that C_L for CO_2 must be less than such values and the concentration of CO_2 in the exit gas $< \sim 10$ –50 mmHg, i. e. $< \sim 1.5$ –6.5 vol.% CO_2 .

How is this to be achieved? A mass balance on CO_2 with CER in mol/m^3 air s gives

$$CER = (Q_G/V)(P/RT)(y_{\text{CO}_2, \text{out}} - y_{\text{CO}_2, \text{in}}) \quad (5.29)$$

Since $y_{\text{CO}_2, \text{in}}$ is essentially zero (0.04 % in air), then

$$CER = (Q_G/V)(P/RT)y_{\text{CO}_2, \text{out}} \quad (5.30)$$

Similarly, a mass balance for OUR gives

$$OUR = (Q_G/V)(P/RT)(y_{O_2, in} - y_{O_2, out}) \quad (5.31)$$

or

$$OUR = (Q_G/V)(P/RT)(0.21 - y_{O_2, out}) \quad (5.32)$$

if only air is sparged. However, since $CER = OUR$, then

$$y_{CO_2, out} = 0.21 - y_{O_2, out} = \Delta y_{O_2} < \sim 0.065 \quad (5.33)$$

in order to keep the pCO_2 low enough to avoid a deterioration in the culture. Since for the same cell density on scale-up, oxygen demand (and therefore OUR) remains the same, from Eqs. 5.31 and 5.32, to hold the mass balances the same, Q_G/V should be held constant, i. e. constant vvm scale-up ensures that if the pCO_2 is acceptable at the small scale, it will remain so at large.

Since constant vvm scale up leads to a linear increase in superficial velocity, v_s , with scale and in industry (Sieblist et al. 2011a), the main concern is the OUR , then because of the perception of the ‘shear’ sensitivity, such an approach is often not followed. There is also a concern for foaming. Because of that perception, scale-up is done at less than constant vvm but since $CER = OUR$ (Eq. 5.27), then

$$y_{CO_2, out} \propto V/Q_G \propto (1/vvm) \quad (5.34)$$

leading to higher pCO_2 levels at the larger scales, which, depending on the flow rate chosen, may lead to a poorer culture performance. Alternatively, the required OUR is obtained by increasing the oxygen concentration to increase the driving force for oxygen-mass transfer. However, from Eq. 5.31, if $y_{O_2, in}$ is increased by using oxygen, oxygen enriched air or back pressure whilst OUR remains the same to meet a particular oxygen demand, then Q_G/V is reduced. Thus from Eqs. 5.27 and 5.30, pCO_2 increases.

Of course, the pCO_2 at the small scale may be much lower than that at which problems occur, especially if a high vvm gas flow rate is used as in the $ambr^{TM}$ as discussed in Sect. 5.9. In that case constant vvm scale-up may not be required. For such a situation, Sieblist et al. (2011a) suggest that a practical experimental approach to the optimization is to first enhance the gas throughput to a value where the pCO_2 concentration is kept within the desired interval (preferably established at the small scale) and then, secondly, to increase the impeller speed (and hence power input) so that in accordance with Eq. 5.23 for the particular media, the k_La is sufficient to cope with the oxygen transfer demands. As discussed below, such an increase in speed is unlikely to damage the cells.

5.3.3 pH and Osmolality

Once dissolved in an aqueous system such as cell culture media, CO_2 can react with different ions in the media, thus giving rise to the lowering of pH which is also detrimental to cell culture. In order to maintain the pH in the desired range, alkaline salts must be added which increases the osmolality and can lead to growth inhibition (de Zengotita et al. 2002; Mostafa and Gu 2003). Thus, if CO_2 mass transfer (stripping) is inadequate, problems may arise from high pCO_2 , pH control issues and high osmolality. It is a critical aspect of large scale, high density animal cell culture (Xing et al. 2009; Nienow 2010).

5.4 Heat Transfer

Even at the high cell densities now being achieved, the actual oxygen uptake rate (*OUR*) is low compared to other types of fermentation. Since metabolic heat release, Q_H (W m^{-3}) is proportional to the *OUR* ($\text{mol O}_2 \text{ m}^{-3} \text{ s}^{-1}$) (Van't Riet and Tramper 1991), i. e.,

$$Q_H = \sim 4.6 \times 10^5 \text{OUR} \quad (5.35)$$

Q_H for animal cell culture is also relatively low. Therefore, though heat release scales with the volume of the reactor, i.e., T^3 whilst cooling surface area scales with T^2 , simple cooling jackets are sufficient for good temperature control even at the commercial scale. Typical operating temperatures are cell line specific and for mammalian cells vary between about 36°C to 38°C whilst for insect cells, it lies between 25°C and 30°C . The agitation intensity itself has little impact on the overall heat transfer coefficient.

5.5 Homogeneity Issues

Even though the agitation intensity required to produce the required *OTR* is relatively gentle (typically $< 0.05 \text{ W/kg}$), the flow in animal cell culture bioreactors from the bench scale and up is turbulent, $Re > \sim 10^4$. Under these conditions, the time required to homogenize the contents of a bioreactor, the mixing time, θ_m is given by

$$\theta_m = 5.9(\bar{\epsilon}_T)_g^{-1/3}(D/T)^{-1/3}T^{2/3} \quad (5.36)$$

for bioreactors for $H = T$ with a single impeller independent of whether it is an axial or radial flow type (Ruszkowski 1994; Nienow 1997a,b). Equation 5.35 has also

recently been shown to fit the mixing time measured at the bench scale using ‘Elephant Ear’ and other axial flow impellers (Simmons et al. 2007). Thus if a similar $(\bar{\epsilon}_T)_g$ is used at different scales in order to achieve the required $k_L a$ values as indicated by Eq. 5.23, mixing time increases with $(\text{scale})^{2/3}$ if geometric similarity is maintained. This increase enhances the inhomogeneity both spatially and temporally on the large scale with respect to the bench in relation to dO_2 , pH and nutrients in fed batch cultures.

For triple impellers in a vessel with an aspect ratio of 3, the equation for mixing time obtained by Cooke et al. (1988) was

$$(\theta_m)_{radial} = 3.3N^{-1}Po_g^{-1/3}(H/D)^{2.43} \quad (5.37)$$

for radial flow impellers spaced T apart with the submergence of the upper impeller, $\sim 2/3 T$. Equation 5.37 can be rearranged to show that with dual impellers too

$$(\theta_m)_{radial} \propto (\bar{\epsilon}_T)_g^{-1/3}T^{2/3} \quad (5.38)$$

i.e. the same increase with scale as for single impellers. For a radial impeller as the lower impeller and one or two down-pumping axial flow impellers, $D/T = 0.5$ above, Cooke et al. (1988) found the constant 3.3 in Eq. 5.37 was reduced by approximately 50 %. Subsequently, Eq. 5.37 was found to fit data well in vessels of aspect ratio 2 with dual, radial flow impellers (Cronin et al. 1994), and suitably modified to a constant of ~ 1.5 , for dual axial flow, high solidity ratio impellers whether up- or down-pumping (Hari-Prajitno et al. 1998). Similar improvements in homogenization have been reported for axial flow impellers and radial-axial combinations (Vrabel et al. 2000; Siebliest et al. 2011b).

The impact of the increased inhomogeneity on increasing scale has been shown to lead to detrimental performance with respect to dO_2 and nutrients (Enfors et al. 2001). The impact also depends on the size of the deviation from the desired controlled value following the addition of pH control chemicals (Osman et al. 2002) and nutrients as well as its duration as indicated by the mixing time. Such excursions can be minimized by sub-surface addition close to the impeller (Langheinrich and Nienow 1999) where the maximum local specific energy dissipation rate, $(\epsilon_T)_{max}$, is found and leads to a rapid local dispersion of the additive (Nienow 2010).

5.6 Choice of Agitation Conditions and Agitator

5.6.1 Mean Specific Energy Dissipation Rate, $\bar{\epsilon}_T$

In order to meet the *OUR* required by achieving an adequate $k_L a$ value, then a sufficiently high energy dissipation rate, $\bar{\epsilon}_T$ has to be imposed by the impeller as shown by Eqs. 5.23, 5.24 and 5.25. The power imposed by an impeller is given by

$$P = P_o \rho N^3 D^5 \quad (5.39)$$

where P_o is the power number, a characteristic of each impeller type. The mean specific energy dissipation rate (or specific power) is given by

$$\bar{\epsilon}_T = P / \rho V \quad (5.40)$$

For the turbulent regime, $Re > \sim 2 \times 10^4$, the power number is constant with values of about 5 for Rushton turbines with lower values for axial flow impellers such as ‘Elephant Ear’ impellers (~ 1.7 (Simmons et al. 2007)) and Lightnin’ A315 hydro-foils (~ 0.85 (Nienow 2010)). P_o can be determined from shaft torque experimentally (Kuboi et al. 1983) or predicted by computational fluid dynamics (CFD) (Nienow et al. 2013a; Werner et al. 2014); or with care, from electric power draw (Nienow et al. 2013a).

In general, when air is sparged into a bioreactor, the level of agitation is able to disperse it and the specific power from agitation falls to an extent which depends on the agitator chosen. Eventually, at a sufficiently high flow rate (which may be as high as 2 vvm), air dispersion by the impeller ceases, at which point the impeller is said to flood. However, in cell culture, at the agitation intensity required to give the desired specific power input to achieve adequate mass transfer, most of the dispersion is provided by the sparger and the impeller has little or no additional effect. Also, the air flow rate is typically around 0.01 vvm and air passes through the impeller region without significantly affecting the flow pattern close to the agitator. As a result, $P_g \approx P$, $P_{O_g} \approx P_o$ and so the mean specific energy dissipation rate under aerated conditions from the impeller during cell culture is essentially equal to $\bar{\epsilon}_T$ (Nienow 2006).

Since Eqs. 5.23–5.25 are independent of impeller type, the implications of this analysis is that for air dispersion and mass transfer, agitator choice is not important.

5.6.2 Hydromechanical Stress Issues Due to Agitation

Clearly, obtaining sufficiently high $k_L a$ values does not impose a problem from the agitation perspective. It is achieved in high cell density fed batch bacterial fermentations where $k_L a$ values up to 800 h^{-1} are required whilst in animal cell culture

they are of the order of $10\text{--}15\text{ h}^{-1}$. The issue is does this agitation intensity lead to deterioration in culture performance or product quality since, because of the lack of a cell wall, animal cells are perceived to be so-called ‘shear-sensitive’? This concept has also led to the development of ‘low shear’ impellers, ones that are marketed as less likely to damage cells.

However, the modern theory of cell damage (Hewitt and Nienow 2007), as with dispersed entities, shows that damage does not occur provided the entity (here the cell) is smaller than the Kolmogorov scale of turbulence, λ_K (Nienow 2010). The Kolmogorov scale can be determined from

$$\lambda_K = (\nu^3 / (\varepsilon_T)_{\max})^{1/4} \quad (5.41)$$

where ν is the kinematic viscosity. It has also been pointed out (Nienow 2010), that for many impellers including the so-called low-shear ‘Elephant Ears’ type (Zhu et al. 2007), the ratio of $(\varepsilon_T)_{\max} / \bar{\varepsilon}_T$ is very similar at the same D/T ratio. Since $\bar{\varepsilon}_T$ is fixed by the k_{LA} required whatever the impeller type, so $(\varepsilon_T)_{\max}$ is also independent of impeller type. Thus, the concept of low and high shear impellers is invalid.

Another concern for damage is related to tip speed. Here there is an anomaly. When impellers are called ‘high shear’, they have high power numbers; conversely, ‘low shear’ have low power numbers. Hence, from Eqs. 5.39 and 5.40, to impart the $\bar{\varepsilon}_T$ value required for mass transfer, ‘low shear’ impellers have to rotate at a higher tip speed than high shear. Thus, based on tip speed, ‘low shear’ impellers are more likely to damage cells than ‘high shear’. The concepts of high and low shear impellers and tip speed as a determinant of ‘shear damage’ are misleading.

Finally, some practitioners consider baffles cause regions of ‘high shear’. However, measurements of local ε_T indicate the value decreases with the distance from the impeller (Wernersson and Tragardh 1999), without any local increase near the baffles (Geisler et al. 1994). Thus, given the advantages of using baffles for improved homogenization and for ensuring an accurate prediction of the requisite $\bar{\varepsilon}_T$ (Nienow 2010), bioreactors with baffles are preferred, especially with increasing scale.

Recently, three different CHO cell lines have been cultivated at $\bar{\varepsilon}_T$ values up to 1 W/kg in turbulent, baffled, bioreactors in work undertaken in Genentech (Nienow et al. 2013b) with dual Rushton turbines and in Novartis (Sieck et al. 2013) with dual ‘Elephant Ear’ impellers. For the three CHO cell lines investigated, the cell density and viability at the bench scale was the same at 1 W/kg as they were in runs undertaken at 0.01–0.02 W/kg as used at the commercial scale. Over the same range of $\bar{\varepsilon}_T$, the antibody quality was also the same and the amount produced was almost unchanged. This insensitivity of cell growth to high agitation intensity fits in well with an earlier review (Nienow 2006) covering TB/C3 mouse hybridomas, EBNA cells, HPV cells, a CHO320 cell line as well as insect cells.

Clearly, it is never possible to prove that all animal cells are equally insensitive to high agitation intensity. Thus, there is always a need to check that the mean specific energy dissipation rate required to achieve satisfactory mass transfer will

not damage the cells on scale up. Given that the flow at the bench and in commercial bioreactors is turbulent, it is also recommended to make that assessment under turbulent flow conditions (Nienow et al. 2013b; Sieck et al. 2013). To allow for the uncertainties concerning large scale turbulent flow structures, each practitioner can decide for themselves what higher value to use. However, Nienow (2014) recommends using an agitator speed at the bench scale ~ 2 times higher than that required to meet the mass transfer needs, equivalent to ~ 10 times increase in $\bar{\epsilon}_T$.

5.7 Hydromechanical Stress from Sparging

Air sparging contributes to the enhancement of $k_L a$ through the value of $v_S g$ chosen in accordance with Eqs. 5.23, 5.24, and 5.25 and also because it adds to $(\bar{\epsilon}_T)_g$

$$(\bar{\epsilon}_T)_g = (\bar{\epsilon}_T) + v_S g \quad (5.42)$$

where g is the gravitational constant and $v_S g$, the mean specific energy dissipation rate from sparging. In addition, increased sparging rates increase the driving force for oxygen uptake and, as explained above, particularly for CO_2 stripping in order to prevent a build up of pCO_2 at the high cell densities produced at the end of cultivation. As a result of the latter, scale-up at approximately constant vvm (typically about 0.01 vvm) is beneficial which leads to a v_S value which increases in proportion to linear scale for geometrically-similar bioreactors.

It has been known for a long time that sparging aeration can destroy animal cells (Handa-Corrigan et al. 1989). This action arises because these cells attach to bubbles (Chalmers and Bavarian 1991) and as they burst at the upper surface of the media, the local stresses on the cells due to bursting (Boulton-Stone and Blake 1993) are many orders of magnitude greater than those due to agitation (Nienow 2006). However, though somehow forgotten, Kilburn and Webb (1968) showed the use of the surfactant, Pluronic F68 at concentrations greater than about 0.5 g L^{-1} acted as a protective agent, due, it was later established, by preventing cell attachment (Chalmers and Bavarian 1991). The use of Pluronic F68 is now ubiquitous to cell culture and generally comes with the media formulation (though occasionally ‘rogue’ poor cultivations have been ascribed to poor quality surfactant).

Nevertheless, the perception of damage due to bursting bubbles still exists and is one of the reasons for using enriched air or oxygen and sparge stones for enhancing mass transfer. However, as reported by Mostafa and Gu (2003), to avoid CO_2 build up using a sparge stone at 0.002 vvm in a 1 m^3 bioreactor, an increase in volumetric air flow rate by a factor of 5 using an open pipe sparger did not damage cells but in fact led to a much improved performance including less foaming. In fact, to the author’s knowledge, there have not been any recent reports in the peer reviewed literature of damage due to bursting bubbles.

However, a problem has been reported by Zhu et al. (2008) at the 10 m³ scale associated with excessively high exit velocities from the holes in a ring sparger. They found that on scale-up at about constant vvm leading to increasing superficial gas velocity, when the local velocity through the sparger holes was $> \sim 30$ m/s, there was a significant decline in NS0 culture performance. By redesigning the ring sparger to give, at the same vvm , hole velocities of ~ 23 m s⁻¹, similar cell density and viability and antibody production were achieved at the 10 m³ scale and at the 0.6 m³. As an initial design consideration, it would seem sensible to maintain sparger exit velocities below ~ 25 m s⁻¹ (Zhu et al. 2008).

5.8 Agitator and Sparger Choice

Since all impellers are equally efficient at achieving mass transfer and have similar $(\epsilon_T)_{\max}/\bar{\epsilon}_T$, the choice does not need to be made in relation to obtaining the desired k_{La} or avoiding ‘shear’ damage. However, it is clear that on scale-up, mixing time is increased but this tendency is mitigated by using axial flow impellers ($D = 0.4\text{--}0.5T$) and relatively low aspect ratio vessels. However, it has been shown that if cell damage does occur due to bursting bubbles, increasing the AR of a bioreactor reduces the proportion of the media in which it takes place (Nienow 2006). If a higher AR is chosen, the use of a second agitator becomes increasingly important at the commercial scale to minimize the increase in inhomogeneities. Thus, aspect ratios up to about 1.2 and dual, wide-blade, high-solidity axial flow impellers with subsurface feeding near the impellers should be selected. Indeed, though air dispersion is not a major consideration as discussed above, with constant vvm scale-up, air dispersion tends to become poorer and up-pumping impellers are better than down pumping in this respect and are thus recommended (Nienow 2010). Open pipe or ring spargers should be used to prevent excessive foaming and pCO₂ and osmolality issues, with exit gas velocities from the sparger being held at $< \sim 25$ m s⁻¹. It is perhaps also worth emphasizing that the sparger should be placed beneath the impeller for the best mass transfer performance.

Finally, in order to follow the protocol recommended above for pCO₂ and dO₂ control, variable speed agitation and sparge rate should be available, capable of giving sufficiently high mean specific energy dissipation rates for oxygen transfer; and air flow for carbon dioxide stripping.

5.9 Scale-up and Ultra Scale-Down Issues

Many of the issues associated with scale-up and scale-down have been addressed already in this chapter. However, recently, there has been a growing interest in increasing the number of clones tested in a selection programme and in order to

handle the numbers, to do so at ever smaller scales (Bareither and Pollard 2011; Pollard 2014). The issue then becomes, does the best culture at this small scale lead to a clone selection which remains the best on scale-up? In addition, in order to handle the number of experiments that it would be desirable to undertake, ideally it requires robotic configurations to be used. Traditionally, such tests have been carried out in shake flasks, but they have a number of issues. They are difficult to control and make measurement in; and they are manually intensive. Also, it has been found that the clones which perform best in the shake flask often do not perform best in a bench scale bioreactor, which is the next step up in scale (Nienow et al. 2013a).

Though many devices have been developed (Bareither and Pollard 2011), the 15 mL ambrTM from TAP Biosystems (Fig. 5.1) seems to have become the most popular, particularly as, like larger scale systems, it uses a variable speed impeller as its energy source and offers fully automated control of pH and dO₂ with the possibility of fed-batch operation. The ambrTM is able to run 24 or 48 parallel cultures at the same time and handle all the steps required for the ~ 14 day process robotically. It has been shown to give very similar cell culture performances (cell density, culture time, productivity and product quality) consistently over all the bioreactors in the ambr system; and equivalent to those in stirred bench scale bioreactors at Genentech (Hsu et al. 2012) and at Merck (Moses et al. 2012), with many other companies reporting similar results at a number of conferences. Interestingly, these publications also showed the cell density achieved and productivity were different (higher!) in shake flasks, though the product quality was the same in all three systems.

Interestingly, the physical mixing and mass transfer characteristics have only recently been reported (Nienow et al. 2013a). They showed that there were a number of physical aspects which are quite different in the ambrTM compared to larger scales. Firstly, the Reynolds number attainable at 1,500 rpm is in the transitional flow regime (~2,500) whilst in other stirred bioreactors from the bench scale up, the flow is turbulent. Also because of the small size of the bioreactor, the air flow, expressed as v_s ($\sim 5 \times 10^{-5} \text{ m s}^{-1}$), is very low. Thus, in order to meet the required *OTR* and give k_La values of up to about 10 h^{-1} , a specific power of up to $\sim 0.4\text{--}0.5 \text{ W kg}^{-1}$ is required. On the other hand, when expressed as *vvm*, the air (or oxygen) flow is high (up to 0.07 vvm). Thus, CO₂ stripping is effective. Finally, the bulk mixing time is enhanced in the transitional region to give times similar to those obtained at the bench scale.

The reasons for which the ambrTM gives results similar to bench scale stirred bioreactors has not been established. It may well be that at the scale of the cell, which is still below λ_K , the mass transfer to and from the cell is purely diffusive. Therefore, good control of dO₂ and pH as found at the bench scale with similar mixing times ensures the cells are exposed to similar environments; and the high *vvm* ensures low pCO₂. Thus, equivalent performances are obtained.

Conclusions

The fundamental theory of mass transfer has been developed and simplified to show how oxygen transfer rates depend on the concentration driving force on the one hand and the mass transfer coefficient, $k_L a$, on the other. The former for the most common type of bioreactor, the stirred vessel from the small 15 mL ambrTM to the largest commercial scales of about 25 m³, is determined by the rate of gas sparging, the gas composition, back and static pressure. The latter, $k_L a$, depends on the specific power input (mean specific energy dissipation rate) from the impeller and the sparged gas; and the superficial gas velocity (the volumetric flow rate divided by the cross-sectional area of the bioreactor) through the bioreactor. For oxygen, which is sparingly soluble in water, the theory can be used to develop simple experimental techniques for measuring $k_L a$ which can be further simplified because the specific oxygen demand of animal cells is low as is the current cell density achievable ($>10^7$ cells mL⁻¹) compared to the oxygen uptake rate with bacterial and mycelial fermentations. This ease of measurement is important because the absolute value of $k_L a$ is very sensitive to the presence of salts (which enhance it relative to water) and antifoams and protective agents such as Pluronic F68 (which reduce it). As a result, accurate correlations from which $k_L a$ can be predicted are not available. At present, the best appears to be that published by Van't Riet (1979) for coalescing systems.

The next mass transfer issue addressed is that of stripping carbon dioxide from the media. Stripping is necessary because for each mol of oxygen utilized by the cells, approximately a mol of CO₂ is produced. However, unlike oxygen, CO₂ is very soluble in aqueous systems and this causes significant difficulties when trying to measure $k_L a$ for CO₂. As a result, incorrect values are often quoted. It is shown that because of the similar values of diffusivity, the $k_L a$ for both gases must be very similar. On the basis of this similarity, it is shown that for effective stripping, sparging at approximately constant vvm across the scales is required.

Achieving effective oxygen transfer and CO₂ stripping is made more difficult from the perceived sensitivity of animal cells to hydromechanical stress from agitation and bursting bubbles. As a result, oxygen transfer is achieved at agitation intensities and sparge rates that are too low by using sparge stones to enhance interfacial area and enriched air or pure oxygen to increase driving force. In turn, this perception has led to problems of pCO₂ build up on scale-up which in turn can cause pH and osmolality issues. Therefore, 'shear sensitivity' in relation to mass transfer is discussed and an operating protocol is proposed to overcome high pCO₂ occurring. This protocol involves increasing the air sparge rate through ring or pipe spargers to strip CO₂ followed by enhancing agitator speed to give the required dO₂. Particularly notable are recent studies which show mean specific energy

(continued)

dissipation rates in stirred bioreactors including the ambr™ up to 0.5 W/kg per impeller have not led to any deterioration in cell growth or product titer or quality.

Since the mean specific energy dissipation rate required for mass transfer normally sets the level used in practice, the other important mixing parameters which are all determined by it are briefly discussed too along with related issues in non-sparged, non-agitated bioreactors.

Nomenclature

<i>a</i>	Specific area of bubbles, m^{-1}
<i>A</i>	Dimensional constant in Eq. 5.23
<i>AR</i>	Aspect ratio, H/T
<i>C_L</i>	Concentration in the liquid phase, mol m^{-3}
<i>d₃₂</i>	Sauter mean diameter, m
<i>D</i>	Agitator diameter, m
<i>D_L</i>	Diffusion coefficient, $\text{m}^2 \text{s}^{-1}$
<i>g</i>	Gravitational constant, 9.81 m s^{-2}
<i>H</i>	Bioreactor fill level, m; or Henry's law constant, $\text{atm. m}^3 \text{ mol}^{-1}$
<i>H_G</i>	Height of aerated liquid, m
<i>J</i>	Rate of mass transfer, mol s^{-1}
<i>k_g</i>	Gas film mass transfer coefficient, $\text{mol s}^{-1} \text{ m}^{-2} \text{ atm}^{-1}$
<i>k_L</i>	Liquid film mass transfer coefficient, m s^{-1}
<i>k_{La}</i>	Specific mass transfer coefficient, s^{-1} or h^{-1}
<i>M</i>	Mass of media, kg
<i>N</i>	Agitator speed, s^{-1} or rpm; or specific rate of mass transfer, $\text{mol m}^{-3} \text{ s}^{-1}$
<i>OD</i>	Oxygen demand, $\text{mol m}^{-3} \text{ s}^{-1}$
<i>OTR</i>	Oxygen transfer rate, $\text{mol m}^{-3} \text{ s}^{-1}$
<i>OUR</i>	Oxygen uptake rate, $\text{mol m}^{-3} \text{ s}^{-1}$
<i>p</i>	Partial pressure, atm
<i>P</i>	Power, W; or total pressure, atm
<i>P_g</i>	Total pressure, atm
<i>P_o</i>	Power number, dimensionless
<i>Q_G</i>	Air flow rate, $\text{m}^3 \text{ s}^{-1}$
<i>Q_H</i>	Heat evolution rate, W m^{-3}
<i>R</i>	Gas constant, $\text{m}^3 \text{ atm K}^{-1} \text{ mol}^{-1}$
<i>Re</i>	Reynolds number, dimensionless
<i>SOD</i>	Specific oxygen demand, $\text{mol s}^{-1} \text{ cell}^{-1}$
<i>t</i>	Temperature, °C; or time, s
<i>T</i>	Bioreactor diameter, m; or absolute temperature, K
<i>v_S</i>	Superficial gas velocity, m s^{-1}

VVM Specific volumetric flow rate, (min^{-1})

V Volume of media, m^3

y Mol fraction, dimensionless

X Cell density, cells m^{-3} ; or % dO_2

Greek Letters

α, β Exponents

ΔC Concentration driving force, mol m^{-3}

ϵ_G Hold-up, dimensionless

ϵ_T Local specific energy dissipation rate, W kg^{-1}

$\bar{\epsilon}_T$ Mean specific energy dissipation rate, W kg^{-1}

λ_K Kolmogoroff turbulence scale, m

μ Viscosity, Pa s

ν Kinematic viscosity, $\text{m}^2 \text{s}^{-1}$

ρ Liquid density, kg m^{-3}

τ_p Time constant of the oxygen probe, s

θ_m Mixing time, s

Subscripts

CO_2 Carbon dioxide

Crit Critical oxygen concentration

I At the interface

In Entering at the sparger

G When air is sparged; or in the gas phase

Max Maximum

Out At the exit

O_2 Oxygen

Superscript

***** At equilibrium

References

- Albaek MO, Gernaey KV, Hansen MS, Stocks SM (2011) Modeling enzyme production with *Aspergillus oryzae* in pilot scale vessels with different agitation, aeration, and agitator types. *Biotechnol Bioeng* 108:1828–1840
- Anderlei T, Büchs J (2001) Device for sterile online measurement of the oxygen transfer rate in shaking flasks. *Biochem Eng J* 7:157–162
- Bandyopadhyay B, Humphrey AE, Taguchi H (1967) Dynamic measurement of the volumetric oxygen transfer coefficient in fermentation systems. *Biotechnol Bioeng* 9:533–544
- Bareither R, Pollard D (2011) A review of advanced small-scale parallel bioreactor technology for accelerated process development: current state and future need. *Biotechnol Prog* 27:2–14
- Betts JPJ, Warr SRC, Finka GB, Uden M, Town M, Janda M, Baganz F, Lye G (2014) Impact of aeration strategies on fedbatch cell culture kinetics in a single use 24 well miniature bioreactor. *Biochem Eng J* 82:105–116
- Boulton-Stone JM, Blake JR (1993) Gas bubbles bursting at a free surface. *J Fluid Mech* 254:103–111
- Chalmers JJ, Bavarian F (1991) Microscopic visualization of insect cell-bubble interactions. ii: the bubble film and bubble rupture. *Biotechnol Prog* 7:151–158

- Cooke M, Middleton JC, Bush JR (1988) Mixing and mass transfer in filamentous fermentations. In: King R (ed) Proceedings of the 2nd international conference of bioreactor fluid dynamics, BHR Group, Cranfield, pp 37–64
- Cooke M, Dawson MK, Moody GW, Whitton MJ, Nienow AW (1991) Mass transfer in aerated agitated vessels; assessment of the NEL/Hickman steady state method. In: Bruxelmann M, Froment G (eds) Proceedings of the 7th European mixing conference, KVIV, pp 409–418
- Cronin DG, Nienow AW, Moody GW (1994) An experimental study of the mixing in a protofermenter agitated by dual Rushton turbines. *Food Bioprocess* 72:35–40
- Davies JT (1972) Turbulence phenomena. Academic, New York
- De Jesus MJ, Wurm FM (2013) Scale-up and predictability in process development with suspension cultures of mammalian cells for recombinant protein manufacture: comments on a trend reversal. *Pharmaceut Bioprocess* 4:333–335
- De Jesus MJ, Girard P, Bourgeois M, Baumgartner G, Jacko B, Amstutz H, Wurm FM (2004) TubeSpin satellites: a fast track approach for process development with animal cells using shaking technology. *Biochem Eng J* 17:217–223
- de Zengotita VM, Schmelzer AE, Miller WM (2002) Characterisation of hybridoma cell responses to elevated pCO₂ and osmolality: intracellular pH, cell size, apoptosis and metabolism. *Biotechnol Bioeng* 77:369–380
- Doig SD, Ortiz-Ochoa K, Ward JM, Baganz F (2005) Characterization of oxygen transfer in miniature and lab-scale bubble column bioreactors and comparison of microbial growth performance based on constant *k_La*. *Biotechnol Prog* 21:1175–1182
- Enfors S-O et al (2001) Physiological responses to mixing in large-scale bioreactors. *J Biotechnol* 85:175–185
- Garnier A, Voyer R, Tom R, Perret S, Jardin B, Kamen A (1996) Dissolved carbon dioxide accumulation in a large scale and high density production of TGF β receptor with baculovirus infected Sf-9 cells. *Cytotechnology* 22:53–63
- Geisler R, Krebs R, Forschner P (1994) Local turbulent shear stress in stirred vessels and its significance for different mixing tasks. In: Proceedings of the 8th European mixing conference. Institution of Chemical Engineers, Rugby, pp 241–251
- Gezork K, Bujalski W, Cooke M, Nienow AW (2001) Mass transfer and hold-up characteristics in gassed, stirred vessels at intensified operating conditions. *Chem Eng Res Des* 79:965–972
- Goudar CT, Matanguihan R, Long E, Cruz C, Zhang C, Piret JM, Konstantinov KB (2007) Decreased pCO₂ accumulation by eliminating bicarbonate addition to high cell-density cultures. *Biotechnol Bioeng* 96:1107–1117
- Handa-Corrigan A, Emery AN, Spier RE (1989) Effects of gas-liquid interfaces on the growth of suspended mammalian cells: mechanisms of cell damage by bubbles. *Enzyme Microb Technol* 11:230–235
- Hari-Prajitno D, Mishra VP, Takenaka K, Bujalski W, Nienow AW, McKemie JM (1998) Gas-liquid mixing studies with multiple up- and down-pumping hydrofoil impellers: power characteristics and mixing time. *Can J Chem Eng* 76:1056–1068
- Heinen JJ, van't Riet K (1982) Mass transfer, mixing and heat transfer phenomena in low viscous bubble column reactors. In: Proceedings of the 4th European conference on mixing, BHRGroup, Cranfield, pp 195–224
- Hermann R, Lehmann M, Büchs J (2003) Characterization of gas-liquid mass transfer phenomena in microtiter plates. *Biotechnol Bioeng* 81:178–186
- Hewitt CJ, Nienow AW (2007) The scale-up of microbial batch and fed-batch fermentation processes. *Adv Appl Microbiol* 62:105–136
- Hoeks FWJMM, Khan M, Guter D, Willems M, Osman JJ, Mommers R, Wayte J (2004) Industrial applications of mixing and mass transfer studies. In: Alvin W Nienow's day; stirred, not shaken symposium. The University of Birmingham, Birmingham
- Hsu W-T, Aulakh RPS, Traul DL, Yuk IH (2012) Advanced microscale bioreactor system: a representative scale-down model for bench-top bioreactors. *Cytotechnology* 64:667–678
- Hu B, Nienow AW, Stitt EH, Pacey AW (2007) Bubble sizes in agitated water-hydrophilic organic solvents for heterogeneous catalytic reactions. *Ind Eng Chem Res* 46:4451–4458

- Kilburn DG, Webb FC (1968) The cultivation of animal cells at controlled dissolved oxygen partial pressure. *Biotechnol Bioeng* 10:801–814
- Kuboi R, Nienow AW, Allsford K (1983) A multipurpose stirred tank facility for flow visualisation and dual impeller power measurement. *Chem Eng Commun* 22:29–39
- Langheinrich C, Nienow AW (1999) Control of pH in large scale, free suspension animal cell bioreactors: alkali addition and pH excursions. *Biotechnol Bioeng* 66:171–179
- Langheinrich C, Nienow AW, Stevenson NC, Emery AN, Clayton TM, Slater NKH (2002) Oxygen transfer in stirred bioreactors under animal cell culture conditions. *Food Bioprod Process* 80:39–44
- Lavery M, Nienow AW (1987) Oxygen transfer in animal cell culture medium. *Biotechnol Bioeng* 30:368–373
- Linek V, Vacek V, Benes P, Sinkule J (1987) Comments on initial response analysis of mass transfer in gas sparged stirred vessels. *Chem Eng Sci* 42:389–390
- Lu W-M, Wu H-Z, Chou C-Y (2002) Gas recirculation rate and its influences on mass transfer in multiple impeller systems with various impeller combinations. *Can J Chem Eng* 80:51–62
- Machon V, Pacek AW, Nienow AW (1997) Bubble sizes in electrolyte and alcohol solutions in a turbulent stirred vessel. *Chem Eng Res Des* 75:339–345
- Martin T, McFarlane CM, Nienow AW (1994) The influence of liquid properties and impeller type on bubble coalescence behaviour and mass transfer in sparged, agitated bioreactors. In: *Proceedings of the 8th European mixing conference, Cambridge, September 1994*. Institution of Chemical Engineers, Rugby, pp 57–64
- Morao A, Maia CI, Fonseca MMR, Vasconcelos JMT, Alves SS (1999) Effect of antifoam addition on gas–liquid mass transfer in stirred fermenters. *Bioprocess Eng* 20:165–172
- Moses S, Manahan M, Ambrogelly A, Ling WLM (2012) Assessment of ambrTM as a model for high-throughput cell culture process development strategy. *Adv Biosci Biotechnol* 3:918–927
- Mostafa SS, Gu X (2003) Strategies for improved dCO₂ removal in large-scale fed-batch cultures. *Biotechnol Prog* 19:45–51
- Nienow AW (1997a) The mixer as a reactor – liquid/solid systems, Chapter 17. In: Hamby N, Edwards MF, Nienow AW (Eds) *Mixing in the process industries*, 2nd edn (paperback revision). Butterworth Heinemann, London, pp 394–411
- Nienow AW (1997b) On impeller circulation and mixing effectiveness in the turbulent flow regime. *Chem Eng Sci* 52:2557–2565
- Nienow AW (2003a) Letter to the editor. *Can J Chem Eng* 81:318
- Nienow AW (2003b) Aeration-biotechnology. In: Kirk Othmer encyclopedia of chemical technology, vol 1, 5th edn. Wiley, New York, pp 730–747
- Nienow AW (2006) Reactor engineering in large scale animal cell culture. *Cytotechnology* 50:9–33
- Nienow AW (2010) Impeller selection: animal cell culture. In: Flickinger MC (ed) *Encyclopedia of industrial biotechnology*, vol 5. Wiley, Hoboken, pp 2959–2971
- Nienow AW (2014) Letter to the editor. *J Biotechnol* 171:82–84
- Nienow AW, Langheinrich C, Stevenson NC, Emery AN, Clayton TM, Slater NKH (1996) Homogenisation and oxygen transfer rates in large agitated and sparged animal cell bioreactors: some implications for growth and production. *Cytotechnology* 22:87–94
- Nienow AW, Rielly CD, Brosnan KM, Bargh N, Lee K, Coopman K, Hewitt CJ (2013a) The physical characterisation of a microscale parallel bioreactor platform with an industrial CHO cell line expressing an IgG4. *Biochem Eng J* 76:25–36
- Nienow AW, Scott WH, Hewitt CJ, Thomas CR, Lewis G, Amanullah A, Kiss R, Meier SJ (2013b) Scale-down studies for assessing the impact of different stress parameters on growth and product quality during animal cell culture. *Chem Eng Res Des* 91:2265–2274
- Oosterhuis NMG, Neubauer P, Junne S (2013) Single-use bioreactors for microbial cultivation. *Pharmaceut Bioprocess* 1:167–177
- Osman JJ, Birch J, Varley J (2002) The response of GS-NSO myeloma cells to single and multiple pH perturbations. *Biotechnol Bioeng* 79:398–407
- Ozturk SS (1996) Engineering challenges in high-density cell culture systems. *Cytotechnology* 22:3–16

- Pedersen AG (1997) k_La characterisation of industrial fermenters. In: Nienow AW (ed) Proceedings of 4th international bioreactor and bioprocess fluid dynamics conference. BHRGroup, Cranfield, pp 263–276
- Pollard D (2014) Are automated disposable small-scale reactors set to dominate the future of pharmaceutical bioprocess development? *Pharmaceut Bioprocess* 2:9–12
- Prins A, van't Riet K (1987) Proteins and surface effects in fermentation: foam, antifoam and mass transfer. *Trends Biotechnol* 5:296–301
- Ruszkowski S (1994) A rational method for measuring blending performance and comparison of different impeller types. In: Proceedings of the 8th European mixing conference. Institution of Chemical Engineers, Rugby, pp 283–291
- Sieblist C, Aehle M, Pohlscheidt M, Jenzsch M, Lübbert A (2010) A test facility for fritted spargers of production-scale-bioreactors. *Cytotechnology* 63:49–55
- Sieblist C, Hägeholz O, Aehle M, Jenzsch M, Pohlscheidt M, Lübbert A (2011a) Insights into large-scale cell-culture reactors: II. Gas-phase mixing and CO₂ stripping. *Biotechnol J* 6:1547–1556
- Sieblist C, Jenzsch M, Pohlscheidt M, Lübbert A (2011b) Insights into large-scale cell-culture reactors: I. Liquid mixing and oxygen supply. *Biotech J* 6:1532–1546
- Sieblist C, Jenzsch M, Pohlscheidt M (2013) Influence of Pluronic F68 on mass transfer. *Biotechnol Prog* 29:1278–1288
- Sieck JB, Cordes T, Budach WE, Rhil MH, Suemeghy Z, Leist C, Villiger TK, Morbidelli M, Soos M (2013) Development of a scale-down model of hydrodynamic stress to study the performance of an industrial CHO cell line under simulated production scale bioreactor conditions. *J Biotechnol* 164:41–49
- Simmons MJH, Zhu H, Bujalski W, Hewitt CJ, Nienow AW (2007) Mixing in bioreactors using agitators with a high solidity ratio and deep blades. *Chem Eng Res Des* 85:551–559
- Sweere APJ, Luyben KCMM, Kossen NWF (1987) Regime analysis and scale-down: tools to investigate the performance of bioreactors. *Enzyme Microb Technol* 9:386
- Takahashi K, Nienow AW (1991) Bubble sizes and coalescence rates in an aerated vessel agitated by a Rushton turbine. *J Chem Eng Jpn* 26:536–542
- Telling RC, Stone L (1964) A method of automatic pH control of a bicarbonate – CO₂ buffer system for the submerged culture of hamster kidney cells. *Biotechnol Bioeng* 6:147–158
- Van't Riet K (1979) Review of measuring methods and results in non-viscous gas–liquid mass transfer in stirred vessels. *Ind Eng Chem Process Des Dev* 18:357–364
- Van't Riet K, Tramper J (1991) Basic bioreactor design. Marcel Dekker, New York
- Varley J, Birch J (1999) Reactor design for large-scale suspension animal cell culture. *Cytotechnology* 29:177–205
- Vasconcelos JMT, Alves SS, Bujalski W, Nienow AW (1997) Spatial characteristics of oxygen transfer in a dual impeller agitated aerated tank. In: Proceedings of the 4th international conference on bioreactor and bioprocess fluid dynamics, Edinburgh. BHR Group, Cranfield, pp 645–660
- Vrabel P, van der Lans RGJM, Luyben KCAM, Boon LA, Nienow AW (2000) Mixing in large scale vessels stirred with multiple radial or radial and axial up-pumping impellers: modelling and measurements. *Chem Eng Sci* 55:5881–5896
- Werner S, Kaiser SC, Kraume M, Eibl D (2014) Computational fluid dynamics as a modern tool for engineering characterization of bioreactors. *Pharmaceut Bioprocess* 2:85–99
- Wernersson ES, Tragardh C (1999) Scale-up of Rushton turbine-agitated tanks. *Chem Eng Sci* 54:4245–4256
- Xing Z, Kenty BM, Li ZJ, Lee SS (2009) Scale-up analysis for a CHO cell culture process in large-scale bioreactors. *Biotechnol Bioeng* 103:733–746
- Zhu H, Simmons MJH, Bujalski W, Nienow AW (2007) Mixing of the liquid phase in a model aerated bioreactor equipped with 'Elephant Ear' agitators using particle image velocimetry. In: Proceedings of the 6th International Conference Multiphase Flow (ICMF 2007). Leipzig, Germany, pp 110–120
- Zhu Y, Cuenca JV, Zhou W, Varma A (2008) NS0 cell damage by high gas velocity sparging in protein-free and cholesterol-free cultures. *Biotechnol Bioeng* 101:751–760